Probing Nuclear Motion by Frequency Modulation of Molecular High-Order Harmonic Generation

Xue-Bin Bian*
State Key Laboratory of Magnetic Resonance and Atomic and Molecular Physics, Wuhan Institute of Physics and Mathematics, Chinese Academy of Sciences, Wuhan 430071, People's Republic of China

André D. Bandrauk
Laboratoire de chimie théorique, Département de Chimie, Université de Sherbrooke, Sherbrooke, Quebéc J1K 2R1, Canada
(Received 17 July 2014; published 7 November 2014)

Molecular high-order harmonic generation (MHOHG) in a non-Born-Oppenheimer treatment of H_2^+, D_2^+, is investigated by numerical simulations of the corresponding time-dependent Schrödinger equations in full dimensions. As opposed to previous studies on amplitude modulation of intracycle dynamics in MHOHG, we demonstrate redshifts as frequency modulation (FM) of intercycle dynamics in MHOHG. The FM is induced by nuclear motion using intense laser pulses. Compared to fixed-nuclei approximations, the intensity of MHOHG is much higher due to the dependence of enhanced ionization on the internuclear distance. The width and symmetry of the spectrum of each harmonic in MHOHG encode rich information on the dissociation process of molecules at the rising and falling parts of the laser pulses, which can be used to retrieve the nuclear dynamics. Isotope effects are studied to confirm the FM mechanism.

DOI: 10.1103/PhysRevLett.113.193901 PACS numbers: 42.65.Ky, 33.80.Rv, 34.50.Gb, 42.25.Hz

High-order harmonic generation (HHG), which is a nonlinear process to generate coherent attosecond (1 as $= 10^{-18}$ s) laser pulses [1], has received a lot of attention recently [2–4]. The mechanism of HHG can be interpreted by a semiclassical three-step model [5–8]. In this model, when atoms and molecules are exposed to intense laser fields, the outer shell electron is freed by tunneling ionization from the ground state initially. Then the free electron is accelerated by the laser fields, and returns to the parent ion to recombine with the ground state and emit HHG photons due to a phase change of the electric fields. This model successfully explains the maximum cutoff energy $I_p + 3.17U_p$ (where I_p is the ionization potential and $U_p = I/4\omega^2$ denotes the ponderomotive energy) of HHG observed in atoms and molecules. Recollision with neighboring ions can result in larger harmonic energies [9,10]. It provides an important tabletop XUV source to investigate ultrafast electronic dynamics [11]. An important feature in HHG is the long plateau structure, which reflects the recollision dynamics of photoelectrons.

However, for molecular high-order harmonic generation (MHOHG), nuclear motion during the ionization and recombination steps plays an important role [12,13]. The recombining electrons can experience a change between the orbital it is originally ionized from and the orbital it is recombining. Consequently, the intensity of the harmonics in the plateau is approximately proportional to the square of modulus of the nuclear correlation function, $C(t) = \int \chi(0,R)\chi(t,R)dR$, where χ is the nuclear wave, t is the traveling time of the free electrons. It was theoretically analyzed by Lein [14] and experimentally confirmed by Baker *et al.* [15] as an amplitude modulation (AM), which encodes the information of intracycle electron-nuclear correlation effects. Alternatively, we present a frequency modulation (FM) effect in this Letter to probe the intercycle dynamics of nuclear motion in MHOHG [4].

FM in HHG mainly results from two effects. One is the propagation effect. During the interaction between laser and atoms and molecules, the ionized electrons change the refractive index of the medium. This propagation effect will lead to a blueshift of both the fundamental laser field and the HHG field [16]. However, if the density of atoms and molecules and the intensity of the laser pulses are low, this effect is negligible. The other effect is due to the rapid change envelope for the ultrashort laser pulses. As an example, Gaussian-like pulses include a rising and a falling part as shown in Fig. 1. On the rising part of the pulses, the effective amplitude of each cycle is larger than that of the previous one, this results in a change of the phase of each harmonic [17]. Intuitively, free electrons gain more energies from the laser fields due to the stronger driving force compared to the previous cycle, which leads to a frequency blueshift in the HHG spectra nonadiabatically [18,19]. In the same way, a redshift occurs on the falling part. This amplitude chirp has a similar effect as frequency chirp [20]. The blueshift in HHG has been studied theoretically [17,21] and experimentally [22–24]. Blueshifts can be achieved easily by using an intense long laser pulse (many cycles) interacting with atoms. When the laser intensity is above the ionization saturation threshold I_s, most of the ionization and HHG signals occur on the rising part of the laser pulses. The HHG signals from the falling part are

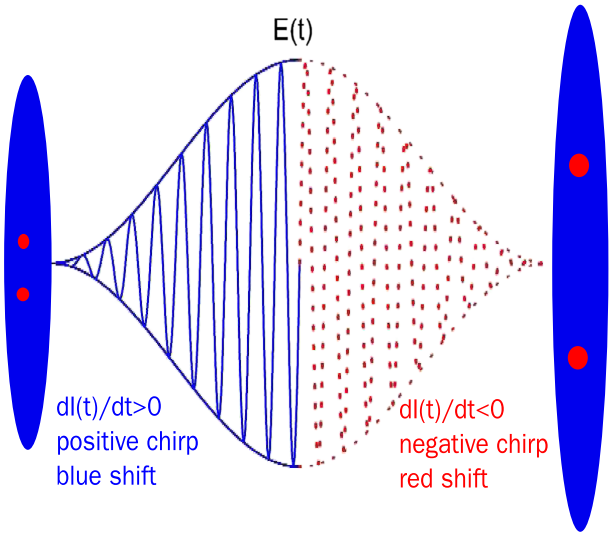

FIG. 1 (color online). Illustration of pulse envelope effect on the shifts of harmonic spectra. The amplitude chirp in the pulse has a similar effect as the frequency chirp [20]. On the rising part of the laser pulse ($t < 0$, solid blue line), $dI(t)/dt > 0$ leads to a blueshift in HHG. On the falling part ($t > 0$, red dotted line), $dI(t)/dt < 0$, which leads to a redshift. At the beginning, the molecule is at its equilibrium distance R_e. However, during the interaction with the laser pulses, the molecule dissociates, leading to larger ionization and more intense spectra on the falling part.

greatly suppressed since no ionization events happen if we neglect the ionization from the ions. As a result, blueshifts induced by the envelope and propagation effects can be well identified in atomic HHG. However, the redshift in HHG on the falling part is difficult to be observed. If the laser intensity is below I_s, the blueshift induced on the rising part of the pulses is comparable to the redshift on the falling part. No obvious net shift in HHG is thus observed. If the laser intensity is above I_s, as discussed above, only net blueshift in HHG can be identified. The redshift of atomic HHG was demonstrated due to the propagation effect depending on the density of the samples [25,26]. To our knowledge, redshift in atomic HHG without considering the propagation effect has not been reported.

Redshift in MHOHG was studied in resonant system HeH^{2+} in fixed-nuclei approximation [27]. This shift is negligible in nonresonant systems as illustrated for H_2^+ in the fixed-nuclei approximation below. In this work, we present a scheme to observe redshifts in MHOHG to probe electron-nuclei correlation in FM rather than AM. As opposed to atomic HHG, one has to include nuclear motion in MHOHG, especially for light molecules. Furthermore, the ionization rate of linear molecules is sensitive to the internuclear distance R. Charge-resonance-enhanced ionization (CREI) has been studied by Zuo and Bandrauk theoretically [28,29] and confirmed experimentally by Gibson *et al.* [30]. For H_2^+, the ionization rate at equilibrium distance $R_e = 2$ a.u. is quite low. However, the ionization rate at the critical internuclear distance R_c may be 2 orders higher than that at R_e [28]. This R dependent ionization provides us an important tool to study molecular dynamics by MHOHG. As illustrated in Fig. 1, the dissociation of molecules makes the signals of ionization and MHOHG stronger on the falling part of the laser pulses, which will induce a strong redshift in MHOHG spectra. Here we study the MHOHG of H_2^+ in a non-Born-Oppenheimer approach (NBOA), which is described below.

We assume the laser field is linearly polarized along the molecular z axis, and the nuclear motion is restricted in one R dimension. The electronic motion is described in three dimensions by cylindrical coordinates (ρ, z, ϕ) [31,32]. After neglecting the center-of-mass motion, due to the cylindrical symmetry of the system, the time-dependent Schrödinger equations (TDSE) can be written as (atomic units are used throughout)

$$i\frac{\partial}{\partial t}\Psi(R,\rho,z,t) = \left[-\frac{1}{2\alpha}\frac{\partial^2}{\partial R^2} - \frac{\nabla_e^2}{2\beta} + V_c - V_I(t)\right]\Psi(R,\rho,z,t), \quad (1)$$

where $\nabla_e^2 = (1/\rho)(\partial/\partial\rho)(\rho(\partial/\partial\rho)) + (\partial^2/\partial z^2)$, $V_c = (Z_1 Z_2/R) - (Z_1/\sqrt{\rho^2 + (z + R/2)^2}) - (Z_2/\sqrt{\rho^2 + (z - R/2)^2})$, and $V_I(t) = [(M_1 - M_2)R/(M_1 + M_2) - (2 + M_1 + M_2)z/(1 + M_1 + M_2)]E(t)$. M_1 M_2 and Z_1 Z_2 are the mass and charge of the two nuclei, respectively. $\alpha = M_1 M_2/(M_1 + M_2)$ and $\beta = (M_1 + M_2)/(M_1 + M_2 + 1)$. In our calculations, the wave function is expanded in a B-spline basis set [33]: $\Psi(R,\rho,z,t) = \sum_{i,j,k} C^{ijk}(t) B_i(R) B_j(\rho) B_k(z)$. The number of B splines in the R, ρ, z directions is 100, 35, and 300, respectively. The total order of the Hamiltonian matrix is 1 050 000. The time-dependent propagation is parallel calculated by a standard Crank-Nicolson method [34]. The initial state is obtained by imaginary propagation methods of the field-free TDSE. The energy of the initial state is $E = -0.59713$ a.u., and the expected equilibrium internuclear distance $\langle R_e \rangle = \langle \Psi | R | \Psi \rangle / \langle \Psi | \Psi \rangle = 2.063$ a.u. The MHOHG spectra are obtained by Fourier transformation of the dipole $d_A(t)$ in acceleration form [4,8].

The laser pulse parameters used in our TDSE calculations are wavelength 800 nm, intensity $I = 3 \times 10^{14}$ W/cm^2. The laser field is expressed as $E(t) = E_0 f(t) \cos(\omega t)$. The envelope of the pulse $f(t)$ is a cosine square shape with total duration $\tau = 20$ cycles, as shown in Fig. 2. The expected value $\langle R(t) \rangle$ of H_2^+ and D_2^+ are also illustrated. One can see that the nuclear motion is almost constant in the first 500 a.u. After that period, due to the ionization of electrons induced by the external laser and the repulsive force between the two nuclei, the molecules start dissociation rapidly. $\langle R(t) \rangle$ is around 2.5 a.u. when the laser intensity is at its peak at $t = 0$ a.u. As calculated in

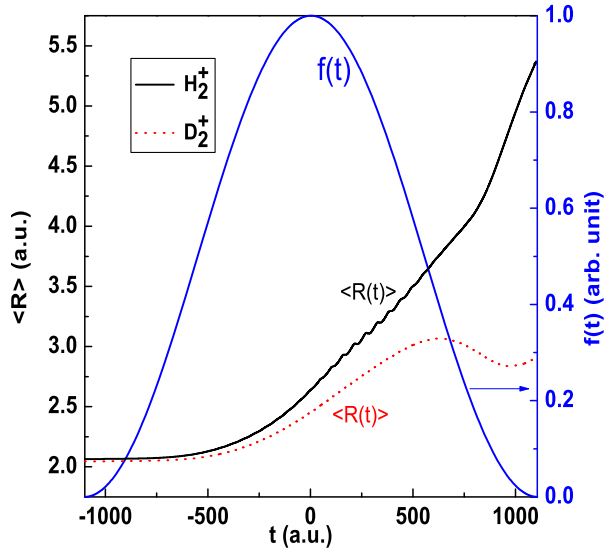

FIG. 2 (color online). Envelope of the laser pulse $f(t)$ and the internuclear distance $\langle R(t)\rangle$ as a function of time. The duration of the laser pulse is 20 cycles in total. The wavelength is 800 nm, and the intensity is $I = 3 \times 10^{14}$ W/cm^2.

Ref. [28], before the internuclear distance R reaches the first critical distance $R_c = 7$ a.u., the ionization rate is proportional to R. We conclude that the ionization and MHOHG signals for $t > 0$ are stronger than that at $t < 0$ since the internuclear distance R is bigger. This imbalance on the falling and rising parts of the laser should lead to net redshifts in MHOHG. We show the MHOHG of H_2^+ in the fixed-nuclei approximation and in the NBOA in Fig. 3.

The MHOHG plateau in the fixed-nuclei approximation exhibits atomiclike HHG structure. Only odd harmonics appear due to the symmetry of the system. The intensity of the each harmonic in the plateau is comparable and the spectral shape of each is symmetric with respect to its central frequency $N\omega$. However, the spectra of MHOHG in the NBOA with nuclear motion are quite different from that in fixed-nuclei approximation. First, the intensity of each harmonic decreases as the harmonic order N increases. This is in agreement with the previous studies [14,15] since the nuclear correlation function reflects the rearrangement of the nuclei, affecting an AM encoding intracycle nuclear dynamics. As a result, it is hard to find the cutoff of MHOHG in NBOA. Second, the overall intensity of MHOHG in NBOA is higher than that in fixed-nuclei approximation. As discussed above, the ionization rate of electron is very sensitive to the internuclear distance R due to CREI [28,29]. The dissociation process will significantly enhance the HHG yield compared to fixed-nuclei approximation as presented in Fig. 3. Third, an important feature is the redshift of the harmonic spectra, which is FM encoding of the correlation between electronic and nuclear dynamics, which has not been addressed previously to our knowledge. The redshift reaches up to the value $\omega/3$ for the laser

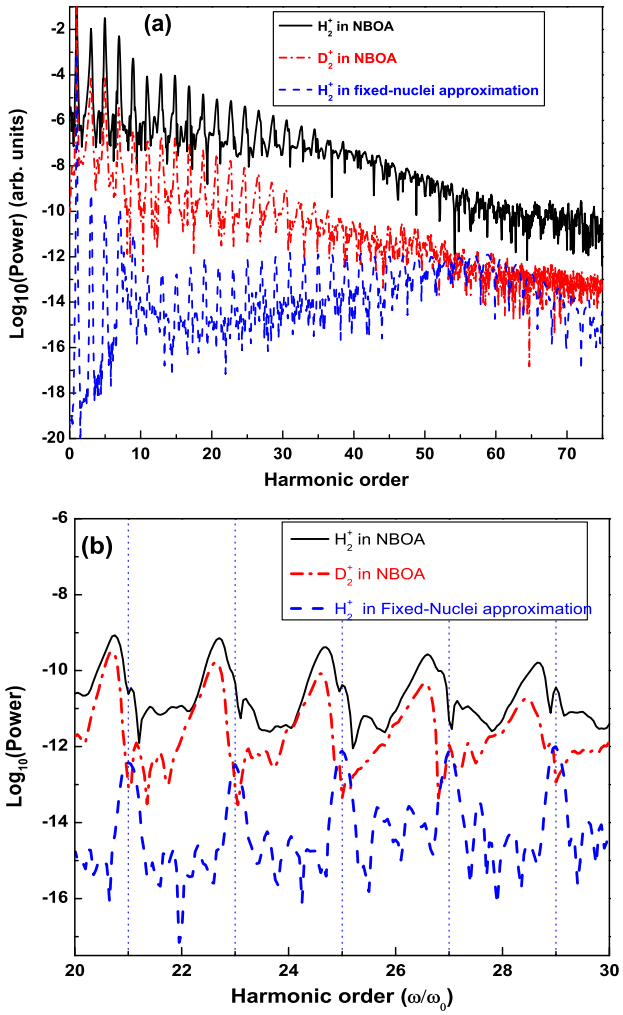

FIG. 3 (color online). MHOHG spectra of H_2^+ and D_2^+ in NBOA calculations and in fixed-nuclei approximation. The laser parameters are the same as those in Fig. 2. In (a), the intensities of harmonics are shifted by 2 orders for clarity. In (b), the intensities of harmonics are not shifted.

parameters used in this work. To further investigate the physics behind the redshifts in MHOHG, the time profile of harmonic ω_N is obtained by a wavelet analysis [35,36]: $d(\omega_N, t) = \int d_A(t) w_{t,\omega_N}(t') dt'$, with the wavelet kernel $w_{t,\omega_N}(t') = \sqrt{\omega_N} W[\omega_N(t' - t)]$ and with mother Morlet wavelet: $W(x) = (1/\sqrt{\sigma}) e^{ix} e^{-x^2/2\sigma^2}$. We calculated the time profile of harmonics with order $N > 20$ as shown in Fig. 4. In fixed-nuclei approximation, the harmonic signals are nearly symmetric to $t = 0$ a.u. However, in NBOA, one can find that most of the harmonic signals are from the falling part of the laser pulse at $t > 0$, thus supporting our analysis.

We also present the isotope effect in NBOA MHOHG, comparing D_2^+ with twice of the mass of H_2^+. The nuclear motion of D_2^+ is slower in the same laser pulse. As illustrated in Fig. 2, the maximal $\langle R(t)\rangle$ is around 3 a.u. for

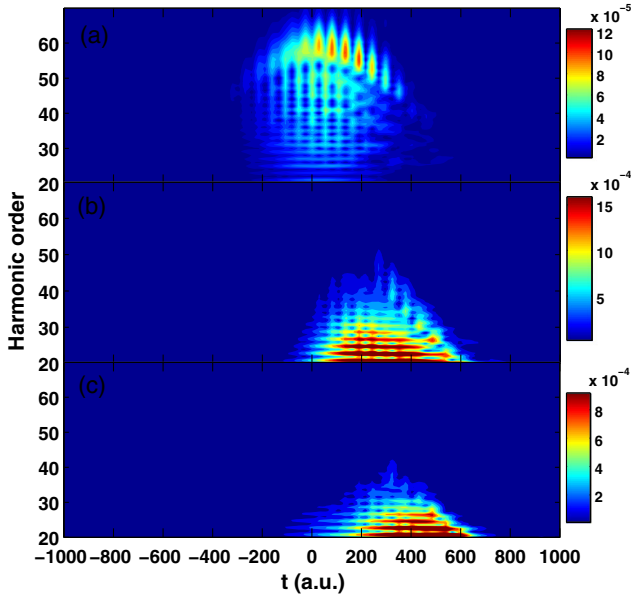

FIG. 4 (color online). Time profile of MHOHG with order $N > 20$. The upper panel is the time profile of MHOHG from H_2^+ in fixed-nuclei approximation, the middle and the lower panels are the time profiles of MHOHG from H_2^+ and D_2^+ in NBOA, respectively.

D_2^+ as compared to 5 a.u. for H_2^+. As a result, the ionization rate of D_2^+ is lower, and the harmonic yield is lower than H_2^+ as illustrated in Fig. 3. However, the spectra of D_2^+ exhibit a larger redshift than that of H_2^+. This can also be explained by investigating the time profile of the MHOHG. From Fig. 4, the peak of the harmonic signals from D_2^+ has a time delay compared to that from H_2^+ due to slower nuclear motion, i.e., occurs later. As a result, the MHOHG of D_2^+ experiences a more rapid change of effective intensity, i.e., $|dI(t)/dt|$ [for the cosine square envelope $f(t)$ used in this work, $|dI(t)/dt|$ is maximal at $t = 550$ a.u.], which leads to a larger redshift in MHOHG. This can also explain that the degree of asymmetry of spectral shape of each harmonic from D_2^+ is higher than that from H_2^+.

The redshift of MHOHG can be used to retrieve the dynamics of nuclear motion. The spectral shift reflects the asymmetry of generated harmonics with respect to $t = 0$ a.u. with peak laser intensity in the time domain. MHOHG is a consequence of ionization; thus, one can use the asymmetry of ionization signals instead of harmonic signals. The relative spectral shift can be roughly expressed as

$$\frac{\Delta\omega}{\omega} = \frac{+\int_{-\tau/2}^{0}\Gamma(R(t),I(t))dt - \int_{0}^{\tau/2}\Gamma(R(t),I(t))dt}{\int_{-\tau/2}^{\tau/2}\Gamma(R_e,I(t))dt}, \tag{2}$$

where Γ is the ionization rate of the system depending on the internuclear distance and laser intensity. The above equation can be further simplified by using average $\bar{R}$ and $\bar{I}$ in the integrals, i.e.,

$$\frac{\Delta\omega}{\omega} = \frac{\Gamma(\bar{R}_1,\bar{I}) - \Gamma(\bar{R}_2,\bar{I})}{2\Gamma(R_e,\bar{I})}. \tag{3}$$

On the rising part of the laser pulse, the nuclear motion in the current laser parameters is small as illustrated in Fig. 2, $\bar{R}_1 \approx R_e$. It is demonstrated that $(\Delta\omega/\omega) \approx -(1/3)$ in Fig. 3(b). From Eq. (3), $\Gamma(\bar{R}_2,\bar{I}) \approx (5/3)\Gamma(R_e,\bar{I})$. If the R dependent ionization rate Γ is known, the internuclear distance R can be retrieved. From Refs. [28,29], Γ is nearly linearly dependent on R before it reaches R_c. As a result, $\bar{R}_2 \approx (5/3)R_3 = 3.3$ a.u., which can qualitatively agree with the TDSE simulations of D_2^+ in Fig. 2 (H_2^+ is Coulomb exploded at the end of the pulse due to higher ionization rate. However, from Fig. 4(b), the HHG signals end at around $t = 600$ a.u. The corresponding internuclear distance is about $R = 3.3$ a.u. as shown in Fig. 2.).

FM is superior to AM in some aspects. AM in MHOHG should be used in the plateau region, since the intensity of HHG decays rapidly in the lower-order perturbative regime and the vicinity of cutoff energy. FM is not restricted to these regions. AM was used in ultrashort laser pulses to probe nuclear motion [14,15] due to intracycle dynamics. FM can be used in a relatively longer pulse for intercycle dynamics. Some inherent physical processes can induce AM in MHOHG. For example, two-center interference [14], resonant harmonic generation [34], may lead to strong AM in MHOHG, which makes it difficult to retrieve nuclei dynamics by AM. FM is comparably stable. Once the internuclear-distance R-dependent ionization rate is known, the nuclei dynamics can be retrieved by FM from the above discussions. The R-dependent ionization rate of multi-electron systems can be well studied by the Hartree-Fock method and density functional theory. FM can potentially be a useful diagnostic tool in attosecond sciences and go beyond single-electron molecules.

In summary, we have theoretically studied the MHOHG from one-electron diatomic molecular ions in intense laser fields in a non-BO treatment to measure the influence of nuclear motion. Not only AM, but also FM encode rich information of electron-nuclear correlation. To our knowledge, this is the first report that the dissociation of molecules will lead to obvious redshifts in FM with intercycle dynamics in harmonic spectra. Usually the ionization rate of stable molecules at the equilibrium distance R_e is very low. When the nuclear distance is far from the R_e, the ionization rate of the system increases rapidly. Consequently, most of the harmonic generation occurs on the falling part of laser pulses, where $dI(t)/dt < 0$, leading to redshifts in MHOHG. This mechanism is confirmed by studying the isotope effect. We have checked our numerical calculations by changing a wide range of wavelength and intensities. The redshift in

MHOHG is not sensitive to the laser parameters provided that the saturation is not achieved and the pulse length is properly adjusted. The mechanism of FM in MHOHG is general, which can be directly applied to other light molecules if the ionization rate is sensitive to nuclear motion. It is hoped that this Letter will stimulate experimental studies in FM.

We thank Jing Zhao, Xiao-Jun Liu, Ming-Hui Yang, Ting-Yun Shi, W. Becker, Y. Pertot, and T. Ozaki for helpful discussions. This work is supported by the National Natural Science Foundation of China (No. 11404376).

*xuebin.bian@wipm.ac.cn

[1] P. B. Corkum and F. Krausz, Nat. Phys. **3**, 381 (2007).
[2] T. Brabec and F. Krausz, Rev. Mod. Phys. **72**, 545 (2000).
[3] M. V. Frolov, N. L. Manakov, T. S. Sarantseva, M. Yu. Emelin, M. Yu. Ryabikin, and A. F. Starace, Phys. Rev. Lett. **102**, 243901 (2009).
[4] A. D. Bandrauk, S. Chelkowski, S. Kawai, and H. Lu, Phys. Rev. Lett. **101**, 153901 (2008).
[5] P. B. Corkum, Phys. Rev. Lett. **71**, 1994 (1993).
[6] K. J. Schafer, B. Yang, L. F. DiMauro, and K. C. Kulander, Phys. Rev. Lett. **70**, 1599 (1993).
[7] M. Lewenstein, P. Balcou, M. Y. Ivanov, A. L'Huillier, and P. B. Corkum, Phys. Rev. A **49**, 2117 (1994).
[8] A. D. Bandrauk, S. Chelkowski, and S. Goudreau, J. Mod. Opt. **52**, 411 (2005).
[9] A. D. Bandrauk, S. Chelkowski, H. Yu, and E. Constant, Phys. Rev. A **56**, R2537 (1997).
[10] M. Lein and J. M. Rost, Phys. Rev. Lett. **91**, 243901 (2003).
[11] T. Popmintchev *et al.*, Science **336**, 1287 (2012).
[12] H. Niikura, F. Légaré, R. Hasbani, A. D. Bandrauk, M. Y. Ivanov, D. M. Villeneuve, and P. B. Corkum, Nature (London) **417**, 917 (2002).
[13] H. Niikura, F. Légaré, R. Hasbani, M. Y. Ivanov, D. M. Villeneuve, and P. B. Corkum, Nature (London) **421**, 826 (2003).
[14] M. Lein, Phys. Rev. Lett. **94**, 053004 (2005).
[15] S. Baker, J. S. Robinson, C. A. Haworth, H. Teng, R. A. Smith, C. C. Chirilă, M. Lein, J. W. G. Tisch, and J. P. Marangos, Science **312**, 424 (2006).
[16] W. M. Wood, C. W. Siders, and M. C. Downer, Phys. Rev. Lett. **67**, 3523 (1991).
[17] C. Kan, C. E. Capjack, R. Rankin, and N. H. Burnett, Phys. Rev. A **52**, R4336 (1995).
[18] K. J. Schafer and K. C. Kulander, Phys. Rev. Lett. **78**, 638 (1997).
[19] M. Geissler, G. Tempea, and T. Brabec, Phys. Rev. A **62**, 033817 (2000).
[20] Z. Chang, A. Rundquist, H. Wang, I. Christov, H. C. Kapteyn, and M. M. Murnane, Phys. Rev. A **58**, R30 (1998).
[21] J. B. Watson, A. Sanpera, and K. Burnett, Phys. Rev. A **51**, 1458 (1995).
[22] H. J. Shin, D. G. Lee, Y. H. Cha, K. H. Hong, and C. H. Nam, Phys. Rev. Lett. **83**, 2544 (1999).
[23] C.-G. Wahlström, J. Larsson, A. Persson, T. Starczewski, S. Svanberg, P. Salières, Ph. Balcou, and A. L'Huillier, Phys. Rev. A **48**, 4709 (1993).
[24] K. Miyazaki and H. Takada, Phys. Rev. A **52**, 3007 (1995).
[25] F. Brandi, F. Giammanco, and W. Ubachs, Phys. Rev. Lett. **96**, 123904 (2006).
[26] F. Giammanco, A. Pirri, F. Brandi, M. Barkauskas, and W. Ubachs, Laser Phys. **15**, 328 (2005).
[27] X. B. Bian and A. D. Bandrauk, Phys. Rev. A **83**, 041403 (2011); **86**, 053417 (2012); Appl. Sci. **3**, 267 (2013).
[28] T. Zuo and A. D. Bandrauk, Phys. Rev. A **52**, R2511 (1995).
[29] T. Seideman, M. Yu. Ivanov, and P. B. Corkum, Phys. Rev. Lett. **75**, 2819 (1995).
[30] G. N. Gibson, M. Li, C. Guo, and J. Neira, Phys. Rev. Lett. **79**, 2022 (1997).
[31] S. Chelkowski, T. Zuo, O. Atabek, and A. D. Bandrauk, Phys. Rev. A **52**, 2977 (1995).
[32] T. Kreibich, M. Lein, V. Engel, and E. K. U. Gross, Phys. Rev. Lett. **87**, 103901 (2001).
[33] R. E. F. Silva, F. Catoire, P. Rivière, H. Bachau, and F. Martín, Phys. Rev. Lett. **110**, 113001 (2013).
[34] X. B. Bian and A. D. Bandrauk, Phys. Rev. A **86**, 053417 (2012); X. B. Bian, Phys. Rev. A **90**, 033403 (2014).
[35] P. Antoine, B. Piraux, and A. Maquet, Phys. Rev. A **51**, R1750 (1995).
[36] C. Chandre, S. Wiggins, and T. Uzer, Physica (Amsterdam) **181D**, 171 (2003).